RESEARCH REPORT ON STRIPED GRAPHENE

Onur Serin
Koç University
Istanbul, Turkey
oserin18@ku.edu.tr

***Supervised by*: Yagiz Morova, Alphan Sennaroglu**
Koç University, Laser Research Laboratory
Istanbul, Turkey
{yamorova}|{asennar}@ku.edu.tr

January 27, 2022

ABSTRACT

Graphene is an effective mode-locker over a wide wavelength range, but it introduces a loss that is significant especially for low-gain lasers due to saturable absorption. A novel way [Optics Letters **45**, 1826 (2020)] to lessen the loss is to use less graphene by using stripes of graphene with gaps in between. In this article, we simulate the effects of such striped graphene layers upon the energy of Gaussian laser beams and their tilted, ellipticized variants. We propose a general formula for energy after passage, and calculate modulation depth.

Graphene has been successfully used as a passive mode-locker, first in multilayer form [1] and then in monolayer form [2] over a wide wavelength range due to independence of absorption from wavelength. However, insertion loss (2.3% per transit for monolayer graphene [2][3]) poses a problem for efficiency, especially for low-gain lasers, and a variety of methods have been proposed to ameliorate the loss. Examples include capacitor structures [4][5] and chemical doping [6], both of which introduce certain drawbacks such as reduction in operational wavelength range and irreversible Fermi level shift, respectively. Such drawbacks have motivated further research on novel techniques, one of which is using femtosecond laser written, zebra patterned graphene layers [7].

Zebra-patterned graphene stripes with gaps in between atop infrasil have the potential to reduce loss while still achieving mode-locking and also allow adjusting the loss by changing gap lengths and translation of the graphene layer [7]. This novel technique raises several questions. What is the energy loss for an incident laser beam and how does it relate to parameters at hand? What is the modulation depth for a striped graphene layer? How does relative position and ablation geometry affect energy output? We have composed a simulation toolkit [8] motivated by such questions to investigate how striped saturable absorbant layers affect the fluence of incident beams. With this toolkit, we have been able to devise a formula to predict energy after passage, and calculate loss and modulation depth both by simulation and proposed formulae. We have also investigated how beam ellipticity and the properties of saturable absorber layers affect the efficacy of predictions.

In the simulation, a laser beam is represented by a square matrix with entries corresponding to fluence values for points on a plane. Each point is unit length away from the adjacent points. For a Gaussian beam, each entry is calculated by Eq.(1), where $J(x, y)$ stands for fluence at (x, y), E_p for the total energy on the plane and w for the radius of the beam waist.

$$J(x, y) := \frac{2E_p}{\pi w^2} e^{\frac{-2}{w^2}(x^2+y^2)} \tag{1}$$

The center of the matrix holds the value for J(0,0). The chosen dimensions of a beam matrix should ensure that the discretized calculation of E_p by Eq.(2) yields a close enough value to actual E_p, which is the result of integrating J(x,y)

of Eq.(1) over the whole plane.

$$E_p \approx \sum_{\text{plane}} J(x,y) \cdot A, \text{ where } A := (\text{unit length})^2 \tag{2}$$

Apart from Gaussian beams, we have also implemented their tilted, ellipticized variants as well. This consideration is useful, as in many cases, a laser beam will shine upon a graphene layer that is tilted to be positioned at the Brewster angle, so that with respect to the graphene plane, the incident beam is ellipticized. Fluence of such beams can be expressed as in Eq.(1a). See that its integration over the whole plane yields E_p, as expected. The angle θ in the equation represents the horizontal tilt of the plane of the graphene layer.

$$J(x,y) := \frac{2E_p \cos(\theta)}{\pi w^2} e^{\frac{-2}{w^2}(x^2 \cos^2(\theta) + y^2)} \tag{1a}$$

A graphene layer is represented by a matrix with entries of 1s and 0s, which stand for presence of graphene at the corresponding location or lack thereof, respectively. The dimensions of a graphene layer matrix is tailored for matching an already initialized laser beam. A layer also has the following associated constants pertaining absorption: α_0 for the linear absorption rate, α_s for the saturable absorption rate, and J_s for the saturation fluence.

A passage of a beam through a layer results in a new beam matrix, by which the new E_p value of the resultant beam can be calculated using Eq.(2). Each J value in the matrix of the passing beam is subject to either of the following operations: It is directly copied to the new beam matrix with the same index, if the corresponding entry on the layer matrix with the same index is 0. Otherwise, the corresponding entry is 1, and Eq.(3) is used to yield the new J value. $\Delta J(J)$ is the loss in fluence function.

$$J_{new} = J - \Delta J(J), \text{ where } \Delta J(J) := J \cdot (\alpha_0 + \frac{\alpha_s}{1 + J/J_s}) \tag{3}$$

Graphene layers of interest for this paper are the ones with a repetitive pattern of stripes of graphene and gaps in between. The width of the graphene stripes and gaps are fixed, represented by d_{gph} and d_{gap} respectively, whereas d_{tot} will stand for $d_{gph} + d_{gap}$ which is the width of one period. The stripes are implemented in the code [8] as being perpendicular to the y axis. Movement along the y axis can be thought of as moving along a column of a beam matrix, whereas the x axis is associated with movement along a row. Sliding of a graphene layer is simulated by instantiating a graphene layer bigger in dimensions than those of the beam matrix that is planned to be acted upon, and new layer matrices with the same dimensions of the beam matrix are created by cropping the bigger one, each time starting at a lower row. The movement at each step is unit length times the number of rows shitfted over. Sliding in other directions is achieved by rotation of the beam matrix, which achieves the desired outcome.

Moving on to proposing of formulae, let us define the parameter R, which stands for the ratio $\frac{d_{gph}}{d_{tot}}$. We can approximate the planar energy after passage by a "miniscule stripes approximation" as in Eq.(4).

$$E_{msa} \approx E_p - R \iint_{-\infty}^{\infty} \Delta J dx dy \tag{4}$$

There is no significant variation depending on the relative position of the graphene layer for $d_{tot} < w$ and Eq.(4) holds regardless of translation in space. This holds for Gaussian beams, as well as their tilted, ellipticized variants that have their major axes parallel to the stripes. As for $d_{tot} > w$, there is considerable variation depending on the position of the

graphene layer, and by dimensional analysis and considering synthesized numerical data, we introduce the following formula:

$$E_{after} \approx E_{msa} \cdot \left[1 + c\frac{d_{tot} - w}{w} \cdot \sin(2\pi \frac{y}{d_{tot}})\right] \tag{5}$$

The variable y in Eq.(5) corresponds to the relative position. When $y = d_{tot}/4$, the center of the beam hits the center of a graphene stripe, resulting in maximum loss. When $y = 3d_{tot}/4$, the center of the beam hits the center of a gapped stripe, resulting in minimum loss. The variation over one period is hypothesized to be sinusoidal and $E_{msa} \cdot c\frac{d_{tot}-w}{w}$ is the variation amplitude, where c is a constant. When the constant c is calibrated for $R \approx 0.5$, it yields accurate results compared to simulations of practical application cases covered by Morova et al. [7]. However, in Eq.(5), there is the problem of not being bounded above as d_{tot} increases when the rest of the parameters stay constant. The variation introduced by translation must converge to a finite value, with the maximum energy value (which is the E_p of the incident beam) corresponding to supposing an all-empty layer and the minimum energy value (E_{min}) calculable by Eq.(4) by supposing a graphene layer with no gaps, i.e. $R = 1$. On top of Eq.(5), we can introduce a clipping condition to overcome this defect as follows: E_{after} values below E_{min} are reassigned as E_{min} and values above incident E_p are reassigned as E_{max}. This suffices for a good fit to simulations for $d_{tot} \gg w$.

Modulation depth can be defined as the percent change from the mean loss to max/min loss for a fixed position of the graphene layer, with E_p, the total energy on the plane being the free variable to alter to get maximum/minimum loss and the rest of the parameters stay constant. We can heuristically argue that the modulation depth M is:

$$M \approx \frac{100}{2}\frac{\alpha_s}{\alpha_s + \alpha_0}\ \% \tag{6}$$

We can proceed as follows: Let E_p^h, E_p^l denote a "very high" and "very low" total energy of the plane for a beam, which will result in minimum and maximum loss respectively by (3). By the approximation of Eq.(4) and taking fluence J on the whole plane to infinity and zero for E_p^h, E_p^l respectively, we get:

$$E_{msa}^h \approx E_p^h - R\alpha_0 E_p^h$$

$$E_{msa}^l \approx E_p^l - R(\alpha_0 + \alpha_s)E_p^l$$

Now, note that we fix an arbitrary position for the graphene layer, and the square bracketed part of (5) is the same for both E_p^h and E_p^l, let us call it β. Thus $E_{after}^h \approx \beta E_{msa}^h$ and $E_{after}^l \approx \beta E_{msa}^l$. The loss ratio for any given configuration is $L := 1 - \frac{E_p - E_{after}}{E_p}$. Then $L^h = \beta R\alpha_0$ and $L^l = \beta R(\alpha_0 + \alpha_s)$. Finally, $M = 100\frac{\text{max L - mean L}}{\text{max L}} \approx 100\frac{L^l - L^h}{2}/L^l = \frac{100}{2}\frac{\alpha_s}{\alpha_s + \alpha_0}$.

Data

By using the simulation and the previous formulae, we can calculate values of interest such as loss, energy over a translative period, modulation depth, and effective saturation fluence. The following data was collected for monolayer graphene unless stated otherwise, whose parameters are taken as $\alpha_0 = 1.61 \times 10^{-2}$, $J_s = 1.45 \times 10^1$ uJcm^{-2}, total absorption loss ratio $= 2.3 \times 10^{-2}$ [3], and we can take $\alpha_s = 2.3 \times 10^{-2} - 1.61 \times 10^{-2} = 6.9 \times 10^{-3}$. For these parameters, Eq.(5) was calibrated by $c = 2 \times 10^{-3}$. For other types of layers, these constants can be tweaked, and the effects of changing graphene parameters on the efficacy of Eq.(5) is investigated at the end.

In the experimental setup of [7], the stripes on the graphene plate were made by laser-micromachining with a fixed ablation thickness of 9.3um, and Gaussian beams were incident to the plate at the Brewster angle for a refractive index of 1.45 for the material. We can calculate how graphene layers of various R with such an ablation thickness vary the energy in different positions to observe whether Eq.(4) and Eq.(5) hold. We take the intracavity beam radius as 34 um, and the total energy on the plane as 3×10^{-4}uJ, which are approximately the values of the experimental setup, and multiply loss by 2 to account for two passes. In Figure 1, the plot on the left shows the calculated variation of the

loss as the focused beam is translated over the layer for R between 10% and 80%. The plot on the right shows the variation of the maximum fractional loss change ($\Delta L/L$, where ΔL is the maximum change in loss as the beam is translated and L is the mean loss) as a function of graphene ablation fraction. We can observe that translation causes a sinusoidal-like change in energy after passage as hypothesized by Eq.(5), and that the position dependence of the graphene layers become negligible for $R > 30\%$, which is concordant with the hypothesis that $d_{tot} < w$ results in negligible translational variance as $d_{tot} \leq 31 < w = 34$um for $R > 30\%$.

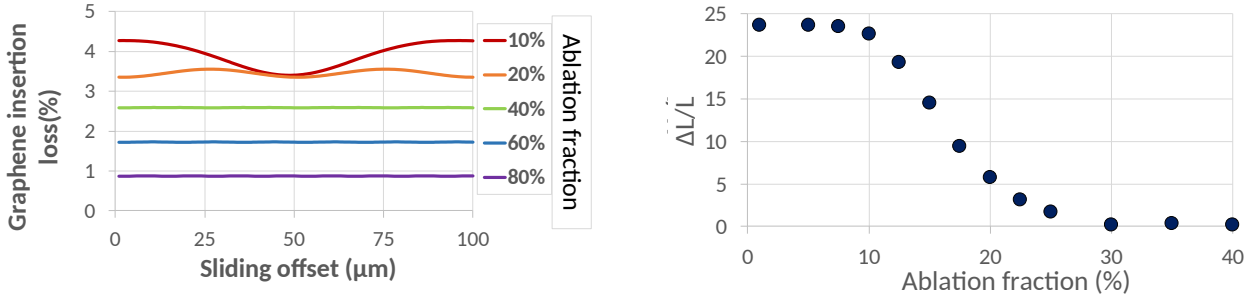

Figure 1: *Left: Calculated variation of loss as the beam is translated over a monolayer graphene for different ablation fractions. Right: Calculated variation of the maximum fractional loss change as a function of ablation fraction. Figure published in [9]*

The percent error table in Figure 2 compares the maxima and minima of the output of Eq.(5) with simulations over a translative period for various example parameters for Gaussian beams. Minus sign indicates overestimation, lack thereof indicates underestimation. The largest absolute error percent value is 0.27%, the average is -0.0082%, and the standard deviation is 0.10. In addition to the cases covered in Figure 2, very low and high graphene ratios of $R = 0.1, 0.9$ and $d_{tot} \approx w$ were also checked to see whether Eq.(5) errs more around their neighborhood, and no significant increase in error percentages overall was observed with those parameters. All these indicate that Eq.(4) and Eq.(5) yield accurate results for energy after passage for Gaussian beams within a margin of error of less than 0.5%, with translational effects taken into account as well.

Calculations of modulation depth using the configurations in Figure 2 with monolayer graphene parameters through scanning in the energy range 10^{-10} uJ $\leq E_p \leq 10^{11}$ uJ concur up to 4 significant figures with the prediction of (6) which asserts that $M \approx 15\%$. This points out that M is independent of w, d_{tot}, R as expected.

We have also calculated percent errors for the ellipticized variants of Gaussian beams tilted at the Brewster angle of infrasil, using the same parameters as in Figure 2. When the major axis is parallel to the stripes, the results are promisingly similar to those in Fig.2. In this case, the largest absolute error percent value is 0.58%, the average is -0.23% (all entries negative except one), and the standard deviation is 0.14. However, for ellipticized Gaussian beams whose major axes are not parallel to the stripes, Eq.(5) needs further adjustment to yield low error results. For the case of major axis being perpendicular to the stripes, swapping w with $w \cdot \tan(\theta_{tilt})$ in Eq.(5) yields low percent errors comparable to the parallel case.

The constant c of Eq.(5) depends on the α_0, α_s and J_{sat} parameters of the saturable absorber layer. As well as affecting c, there is a peculiarity introduced by high α_0 and α_s values. While keeping other parameters the same, increasing α_0 or α_s linearly decreases the average resultant E_p, and this decrease is stronger for α_0. This means that using Eq.(4),(5) will result in more error as α_0 or α_s is taken higher and higher, and there seems to be no simple way of estimating the shift precisely for a given set of parameters. However, this is not a serious issue as the effect is minimal for practical cases dealing with graphene. Even at a very high non-saturable loss of $\alpha_0 = 0.15$, the shift of the average with respect to the estimated one (by Eq.(5)) is on the order of 0.1% (while keeping α_0 small), and a very high saturable loss of $\alpha_0 = 0.15$ introduces an even smaller shift (while keeping α_s small).

Finally, note that the constant c can be calibrated for saturable absorber layers other than monolayer graphene. For example, we can use the following constants for double-layer graphene: $\alpha_0 = 3.05 \times 10^{-2}$, $J_s = 2.25 \times 10^{1}$ uJcm^{-2},

E_p	w	d_{tot}	$\%_{gph}$	@max	@min
$1.0 \cdot 10^{-1}$	20	40	0.3	0.019	-0.050
$1.0 \cdot 10^{-1}$	20	40	0.7	0.012	-0.062
$1.0 \cdot 10^{-3}$	20	40	0.3	0.026	-0.051
$1.0 \cdot 10^{-3}$	20	40	0.7	0.026	-0.056
$1.0 \cdot 10^{-3}$	20	50	0.3	0.061	-0.12
$1.0 \cdot 10^{-3}$	20	50	0.7	0.091	-0.092
$1.0 \cdot 10^{-3}$	30	40	0.3	-0.020	0.020
$1.0 \cdot 10^{-3}$	30	40	0.7	-0.018	0.020
$1.0 \cdot 10^{-3}$	30	50	0.3	0.0059	-0.0076
$1.0 \cdot 10^{-3}$	30	50	0.7	0.0097	-0.0070
$1.0 \cdot 10^{-5}$	20	40	0.3	0.11	-0.15
$1.0 \cdot 10^{-5}$	20	40	0.7	0.11	-0.16
$1.0 \cdot 10^{-5}$	20	50	0.3	0.18	-0.27
$1.0 \cdot 10^{-5}$	20	50	0.7	0.22	-0.24
$1.0 \cdot 10^{-5}$	30	40	0.3	0.011	0.0011
$1.0 \cdot 10^{-5}$	30	40	0.7	0.021	0.0092
$1.0 \cdot 10^{-5}$	30	50	0.3	0.069	-0.058
$1.0 \cdot 10^{-5}$	30	50	0.7	0.081	-0.051

Figure 2: *Percent error table for Eq.*(5) *with respect to the resultant E_p values of Gaussian beams, max and min refer to the maxima and minima for one translative period. Units are uJ, um*

total absorption loss ratio $= 4.6 \times 10^{-2}$ [3], and we can take $\alpha_s = 0.046 - 0.0305 = 1.55 \times 10^{-2}$. The percent error values in Fig.1 has also been calculated for the same parameters for the double-layer graphene case by calibrating the constant c to $c = 4 \times 10^{-3}$. The largest absolute error percent value is 0.55%, the average is -0.017%, and the standard deviation is 0.20.

In this paper, only stripes have been considered due to their ease of manufacturing, but other geometries such as circular patterns could yield interesting properties as well, and they can be readily investigated by extending the layer initialization part of the simulation code.

References

[1] H. Zhang, D.Y. Tang, L.M. Zhao, Q.L. Bao, and K.P. Loh, "Large energy mode locking of an erbium-doped fiber laser with atomic layer graphene," Optics Express **17**, 17630–17635 (2009).

[2] C.C. Lee, G. Acosta, J.S. Bunch, and T.R. Schibli, "Mode-locking of an Er:Yb:glass laser with single layer graphene," International Conference on Ultrafast Phenomena, TuE29 (2010).

[3] W.B. Cho, J.W. Kim, H.W. Lee, S. Bae, B.H. Hong, S.Y. Choi, I.H. Baek, K. Kim, D. Yeom, and F. Rotermund, "High-quality, large-area monolayer graphene for efficient bulk laser mode-locking near 1.25um," Optics Letters **36**, 4089–4091 (2011).

[4] C.C. Lee, S. Suzuki, W. Xie, and T.R. Schibli, "Broadband graphene electro-optic modulators with sub-wavelength thickness," Optics Express **20**, 5264–5269 (2012).

[5] I. Baylam, M.N. Cizmeciyan, S. Ozharar, E.O. Polat, C. Kocabas, and A. Sennaroglu, "Femtosecond pulse generation with voltage-controlled graphene saturable absorber," Optics Letters **45**, 5180–5183 (2014).

[6] H. Liu, Y. Liu, and D. Zhu, "Chemical doping of graphene," Journal of Materials Chemistry **21**, 3335–3345 (2011).

[7] Y. Morova, J.E. Bae, F. Rotermund, and A. Sennaroglu, "Laser-micromachined zebra-patterned graphene as a mode locker with adjustable loss," Optics Letters **45**, 1826–1829 (2020).

[8] O. Serin, "Simulation Toolkit for Laser Beams Masked by Semi-ablated Saturable Absorbant Surfaces," (2020) https://github.com/serinos/beam-graphene/

[9] Y. Morova, O. Serin, J.E. Bae, F. Rotermund, and A. Sennaroglu, "Femtosecond Pulse Generation Using Laser Written Zebra Patterned Graphene with Adjustable Loss," Laser Congress 2020 (ASSL, LAC), Paper JTh2A.28 (2020).